Description of ^{4}He tetramer bound and scattering states

Rimantas Lazauskas*

Groupe de Physique Théorique, Institut de Physique Nucléaire, F-91406 Orsay Cedex, France

Jaume Carbonell†

Laboratoire de Physique Subatomique et de Cosmologie, 53, Avenue des Martyrs, 38026 Grenoble Cedex, France

Faddeev-Yakubovski equations are solved numerically for ^{4}He tetramer and trimer states using realistic helium-helium interaction models. We describe the properties of ground and excited states, and we discuss with a special emphasis the ^{4}He-^{4}He$_3$ low energy scattering.

PACS number(s): 34.50.−s, 21.45.+v, 36.90.+f

I. INTRODUCTION

A helium atom is one of the simplest few-body systems. Nowadays, its structure can be described theoretically with an accuracy better than the spectroscopy one [1]. In spite of this simplicity, the compounds of helium atoms display a series of unique microscopic and macroscopic physical phenomena.

The closed shell electronic structure, as well as the compactness of the helium atom, makes it the most chemically inert noble gas. Nevertheless, the very weak van der Waals attraction between two distant He atoms is responsible for the fact that at very low temperatures, both bosonic ^{4}He and fermionic ^{3}He liquify. In addition, the extreme weakness of the He-He interaction is decisive in explaining why liquid helium is the only known superfluid.

As exciting is the physics of the atomic helium nanoscopic structures (He multimers), recent inspiring experiments [2,3] have demonstrated the existence of bound diatomic ^{4}He systems (dimers)—the ground state with the weakest binding energy of all naturally existing diatomic molecules. Moreover, a diffraction experiment projecting a molecular beam of small He clusters on nanostructured transmission gratings, allowed a direct measurement of the dimer average bond length value $\langle R \rangle = 52 \pm 4$ Å. Such a large bond, compared to the effective range of the He-He potential, enables one to estimate its binding energy $E \approx \frac{\hbar^2 \langle R \rangle^2}{4m} = 1.1 + 0.3/-0.2$ mK, as well as the ^{4}He-^{4}He scattering length $a_0 = 104 + 8/-18$ Å.

The extreme weakness of the ^{4}He dimer binding energy requires a precise theoretical description of the *ab initio* He-He potential, which results from subtracting the huge energies of separated atoms. Nevertheless, several very accurate theoretical models [4–9] were recently constructed, predicting helium properties in full agreement with experiments. These effective He-He potentials are dominated by the strong repulsion (hard-core) at distances $R_{\text{He-He}} \lesssim 2$ Å, where the

two He atoms are "overlapping." At larger He-He distances, the weak van-der-Waals attraction takes over, creating a shallow attractive pocket with a maximal depth of $V_0 \approx 10.9$ K, centered at $R_{\text{He-He}} \approx 3$ Å. The strong repulsion of the He-He potential at short distance, allows one to treat accurately atomic He systems without having to take into account the internal structure of single He atoms.

The physics of small He clusters is an outstanding laboratory for testing different quantum mechanical phenomena. The bound state of ^{4}He dimer, at practically zero energy, suggests the possibility of observing an Efimov-like state in the triatomic compound [10]. The existence of this ^{4}He dimer bound state very close to threshold is also responsible for a resonant ^{4}He-^{4}He S-wave scattering length $a_0 \approx 104$ Å, which is more than 30 times larger than the typical length scale given by the van der Waals interaction $l \sim 3$ Å. The small He clusters low energy scattering observables should therefore be little sensitive to the details of He-He interaction and should thus exhibit some universal behavior. This sharp separation of different scales can be exploited, making He multimers a perfect test ground for effective field theory (EFT) approaches [11–14].

We present in this work a rigorous theoretical study of the smallest ^{4}He clusters. There exist in the literature a large number of theoretical calculations on triatomic ^{4}He (trimer) [15–17]. However, the four-atomic ^{4}He system (tetramer), being by an order of magnitude more complex in its numerical treatment, remains practically unexplored. Our study tries to fill up this gap by providing original calculations for tetramer bound and scattering states. In addition, some existing ambiguities in triatomic ^{4}He calculations [18] are discussed.

To describe ^{4}He tetramer, Faddeev-Yakubovski (FY) equations in configuration space are solved. In some cases, this method may be cumbersome and numerically expensive. It constitutes nevertheless a very general and mathematically rigorous tool, with a big advantage over many other techniques, that it enables a systematic treatment of bound and continuum states.

The paper is structured as follows: in Sec. II we present the theoretical framework used; in Sec. III we highlight our ^{4}He trimer results. Section IV deals with four-atomic helium systems and in Sec. V, we discuss the possible existence of the rotational states in three-atomic and four-atomic ^{4}He systems. Section VI concludes this work with the final remarks.

*Electronic address: lazauskas@lpsc.in2p3.fr; URL: http://lpscwww.in2p3.fr/theo/Lazauskas/Eng/home.htm

†Electronic address: carbonell@lpsc.in2p3.fr; URL: http://lpscwww.in2p3.fr/theo/Carbonell/Jaume.html

To describe the interaction between the helium atoms, we have used the potential developed by Aziz and Slaman [4], popularly referred to as LM2M2 potential. There exists several equivalent interaction models. However, they all have similar structure and quantitatively provide very close results [17,19].

All results presented in this paper are restricted to the bosonic ^{4}He isotope; therefore in the following, we omit the mass number 4 and refer to ^{4}He as He. All calculations use $\frac{\hbar^2}{m} = 12.12$ K Å^2 as the input mass of He atoms.

II. THEORETICAL FRAMEWORK

A. Faddeev-Yakubovski equations

The Schrödinger equation is the paradigm of nonrelativistic quantum mechanics. However, this equation is not able to separate different rearrangement channels in the asymptote of multiparticle wave function (w.f.). Thus it does not provide explicitly a way to implement the physical boundary conditions for scattering w.f., which are necessary to obtain a unique solution. Faddeev [20] have succeeded to show that these equations can be reformulated by introducing some additional physical constraints, what leads to mathematically rigorous and unique solution of the three-body scattering problem. Faddeev's pioneering work was followed by Yakubovsky. In [21], the systematic generalization of Faddeev equations for any number of particles was presented.

One should mention that the Schrödinger equation may still be applied when solving the few-particle bound state problem. However, then one must deal directly with the total systems w.f., which is fully (anti)symmetric and has quite a complicated structure. Exploiting the knowledge of systems symmetry one often tries to decompose this w.f. into only partially (anti)symmetrized components, which have a simpler structure and are more tractable numerically. One practical way is to decompose systems w.f. into so-called FY components. Then FY equations often have an obvious advantage over the Schrödinger one, since it deals directly only with FY components and avoids construction of a full system wave function.

In what follows, we describe only four-particle FY equations; three-particle Faddeev equations are self-contained in four-particle ones. The calculations presented in this work were performed using the framework of differential FY equations developed by Merkuriev and Yakovlev [22,23]. The major step in these equations is the representation of the systems w.f. as a sum of 18 components: 12 of type K, describing the asymptotic behavior of different 3+1 particle channels, and 6 of type H, describing the systems decomposition into two clusters of two particles:

$$\Psi = \sum_{i<j} K^l_{ij,k} + \sum_{i<j,k<l} H_{ij,kl}. \qquad (1)$$

Here $(ijkl)$ indicates cyclic permutation of particle indices (1234) (see Fig. 1). These FY components are coupled by 18 FY equations. Since all particles are identical, several straightforward symmetry relations can be established between different FY components. Using these relations, the
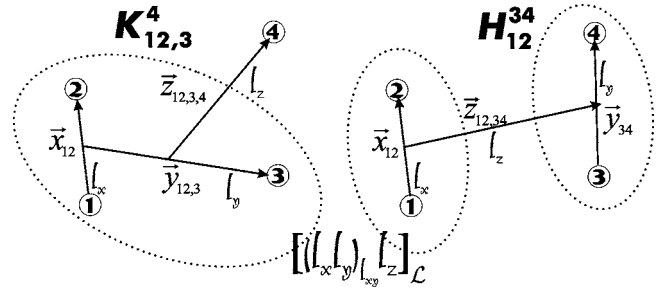
FIG. 1. Faddeev-Yakubovsky components K and H. Asymptotically, as $z \to \infty$, components K describe 3+1 particle channels, whereas components H contain asymptotic states of 2+2 channels.

number of independent FY equations and components reduces to two:

$$(E - \hat{H}_0 - \hat{V})K^4_{12,3} = \hat{V}(P^+ + P^-)[(1 + \varepsilon P_{34})K^4_{12,3} + H_{12,34}],$$

$$(E - \hat{H}_0 - \hat{V})H_{12,34} = \hat{V}\tilde{P}[(1 + \varepsilon P_{34})K^4_{12,3} + H_{12,34}]. \qquad (2)$$

Here $P^+ = P_{12}P_{23}$, $P^- = P_{23}P_{12}$, and $\tilde{P} = P_{13}P_{24}$ are particle permutation operators. $\hat{H}_0$ is the kinetic energy operator of the system and $\hat{V}$ is the potential energy operator for the particle pair (12). The coefficient ε is a Pauli factor: $\varepsilon = 1$ for bosonic systems and $\varepsilon = -1$ for systems of identical fermions.

By applying a combination of permutation operators to the FY components of Eq. (1), one can express the w.f. of the system by means of two nonreducible FY components:

$$\Psi = [1 + (1 + P^+ + P^-)\varepsilon P_{34}](1 + P^+ + P^-)K^4_{12,3} + (1 + P^+$$

$$+ P^-)(1 + \tilde{P})H_{12,34}. \qquad (3)$$

It is convenient to treat Eq. (2) using relative reduced coordinates. These coordinates are proportional to well-known Jacobi coordinates, which are simply scaled by the appropriate mass factors. We use two different sets of relative reduced coordinates, defined as follows:

$$\vec{x}_{ij} = \sqrt{2\frac{m_i m_j}{m_i + m_j}}(\vec{r}_j - \vec{r}_i),$$

$$\vec{y}_{ij,k} = \sqrt{2\frac{(m_i + m_j)m_k}{m_i + m_j + m_k}}\left(\vec{r}_k - \frac{m_i\vec{r}_i + m_j\vec{r}_j}{m_i + m_j}\right),$$

$$\vec{z}_{ijk,l} = \sqrt{2\frac{(m_i + m_j + m_k)m_l}{m_i + m_j + m_k + m_l}}\left(\vec{r}_l - \frac{m_i\vec{r}_i + m_j\vec{r}_j + m_k\vec{r}_k}{m_i + m_j + m_k}\right) \qquad (4)$$

for K-type FY components. m_i and $\vec{r}_i$ are, respectively, the ith particle mass and position vector. To describe H-type com-

ponents, another set of coordinates is more appropriate:

$$\vec{x_{ij}} = \sqrt{2\frac{m_i m_j}{m_i + m_j}}(\vec{r}_j - \vec{r}_i),$$

$$\vec{y_{kl}} = \sqrt{2\frac{m_k m_l}{m_k + m_l}}(\vec{r}_l - \vec{r}_{ki})$$

$$\vec{z_{ij,kl}} = \sqrt{2\frac{(m_i+m_j)(m_k+m_l)}{m_i+m_j+m_k+m_l}}\left(\frac{m_k\vec{r}_k+m_l\vec{r}_l}{m_k+m_l} - \frac{m_i\vec{r}_i+m_j\vec{r}_j}{m_i+m_j}\right).$$

(5)

Using these coordinates, the kinetic energy operator is expressed as a simple sum of Laplace operators:

$$H_0 = -\frac{\hbar^2}{2m}\Delta_R - \frac{\hbar^2}{m}(\Delta_x + \Delta_y + \Delta_z).$$

(6)

Another big advantage of these coordinate sets is the fact that the degrees of freedom due to the center of mass motion are separated.

The dimension of the problem can be further reduced by using the fact that an isolated system conserves its total angular momentum $\mathcal{J}$ and one of its projections $\mathcal{J}_z$. We deal with systems of bosonic He atoms in their ground state, which have a total spin equal to zero. In this case, the system w.f. is independent of the spin and the orbital angular momentum is conserved separately. Using this fact, we expand FY components on a partial-wave basis (PWB) of orbital angular momentum and, omitting the spin:

$$K_{ij,k}^l(\vec{x},\vec{y},\vec{z}) = \sum_{\alpha=(l_x,l_y,l_{xy},l_z)} \frac{\mathcal{F}_\alpha^K(x,y,z)}{xyz}[[Y_{l_x}(\hat{x}) \otimes Y_{l_y}(\hat{y})]_{l_{xy}}$$
$$\otimes Y_{l_z}(\hat{z})]_{\mathcal{L}\mathcal{L}_z},$$

$$H_{ij,kl}(\vec{x},\vec{y},\vec{z}) = \sum_{\alpha=(l_x,l_y,l_{xy},l_z)} \frac{\mathcal{F}_\alpha^H(x,y,z)}{xyz}[[Y_{l_x}(\hat{x}) \otimes Y_{l_y}(\hat{y})]_{l_{xy}}$$
$$\otimes Y_{l_z}(\hat{z})]_{\mathcal{L}\mathcal{L}_z}.$$

(7)

In this basis, the kinetic energy operator reads

$$\hat{H}_0 = \frac{\hbar^2}{m}\left[-\partial_x^2 - \partial_y^2 - \partial_z^2 + \frac{l_x(l_x+1)}{x^2} + \frac{l_y(l_y+1)}{y^2} + \frac{l_z(l_z+1)}{z^2}\right].$$

In Eq. (7), we have introduced the so-called FY amplitudes $\mathcal{F}_\alpha^K(x,y,z)$ and $\mathcal{F}_\alpha^H(x,y,z)$, which are continuous functions in radial variables x, y, and z. The symmetry properties of the w.f. with respect to the exchange of two He atoms impose additional constraints. One should have amplitudes only with an even value of the angular momentum l_x, whether these amplitudes are derived from K or H FY components.

In addition, for H-type amplitudes $\mathcal{F}_\alpha^H(x,y,z)$, the angular momentum l_y should be even as well. The total parity of the system Π is given by $(-)^{l_x+l_y+l_z}$ independently of the coupling scheme (K or H) used.

By projecting Eq. (2) to the PWB of Eq. (7), a system of coupled integrodifferential equations is obtained. In general,

PWB is infinite and one obtains thus an infinite number of coupled equations. This obliges us, when solving these equations numerically, to make additional truncations by considering only the most relevant amplitudes, namely those which have the smoothest angular dependency (small partial angular momentum values l_x, l_y, and l_z).

B. Boundary conditions

Equations (2) are not complete: they should be supplemented with the appropriate boundary conditions for FY components. It is usual to write boundary conditions in the Dirichlet form, which at the origin should mean vanishing FY components. However, the existence of a large strong repulsion region (hard-core) corresponding to the inner part of He-He potential brings additional complications. The relevant matrix elements from the physical interaction region (shallow attractive well) fade away in front of the huge repulsive hard-core terms, thus resulting in severe numerical instabilities.

However, such a strong repulsion at the origin simply indicates that two He atoms cannot get arbitrarily close to each other: for a repulsive region of characteristic size r_h, the probability that two particles get closer to each other at a certain distance $r=c<r_h$ will be vanishingly small. It means that the w.f. of the system vanishes in part of a four-particle space, inside six multidimensional surfaces $r_{ij}=c$, where r_{ij} is the distance between particle i and j. The most straightforward way to improve numerical stability would be to avoid calculating the solution in at least part of the strong repulsion region, and to impose by hand the wave function to be equal to zero in this region. Nevertheless, due to the complex geometry of this domain in the nine-dimensional space of particle relative coordinates, this method is not easy to put into practice.

A nice way to overcome this difficulty was proposed by Motovilov and Merkuriev [24]. The authors showed that an infinitely repulsive interaction at $r_{ij} \leq c$ generates boundary conditions for the FY components which can be ensured by setting

$$(E - \hat{H}_0 - \hat{V})K_{12,3}^4 = 0 \quad \text{for } x < c \qquad (8)$$
$$(E - \hat{H}_0 - \hat{V})H_{12,34} = 0$$

and

$$K_{12,3}^4 + (P^+ + P^-)[(1+\varepsilon P_{34})K_{12,3}^4 + H_{12,34}] = 0$$
$$H_{12,34} + \widetilde{P}[(1+\varepsilon P_{34})K_{12,3}^4 + H_{12,34}] = 0 \quad \text{for } x = c. \qquad (9)$$

In addition, FY components asymptotic behavior should be conditioned as well. For the bound state problem, the w.f. of the system is compact, therefore the regularity conditions can be completed by forcing the amplitudes $\mathcal{F}_\alpha^{K(H)}$ to vanish at the borders of the hypercube $[0,X_{max}] \times [0,Y_{max}] \times [0,Z_{max}]$, i.e.,

$$\mathcal{F}_\alpha^{K(H)}(X_{max},y,z) = \mathcal{F}_\alpha^{K(H)}(x,Y_{max},z) = \mathcal{F}_\alpha^{K(H)}(x,y,Z_{max}) = 0.$$

(10)

In the case of elastic atom-trimer $(1+3)$ scattering, the asymptotic behavior of the w.f. can be matched by simply imposing at the numerical border $z=Z_{max}$, the solution of the $3N$ bound state problem for all the quantum numbers, corresponding to the open channel α_a. It is worth reminding that only K-type components contribute in describing $3+1$ particle channels:

$$\mathcal{F}^K_{\alpha_a}(x,y,Z_{max}) = f_{\alpha_a}(x,y). \tag{11}$$

Indeed, below the first inelastic threshold, at large values of z, the solution of Eq. (2) factorizes into a He trimer ground state w.f.—being a solution of $3N$ Faddeev equations—and a plane wave propagating in the z direction with the momentum $k_{\alpha_a} = \sqrt{\frac{m}{\hbar^2}(E_{cm}-E_{He_3})}$. One has

$$\mathcal{F}^K_{\alpha_a}(x,y,z) \sim f^K_{\alpha_a}(x,y)[\hat{j}_{l_z}(k_{\alpha_a}z) + \tan(\delta)\hat{n}_{l_z}(k_{\alpha_a}z)].$$

Here the functions $f^K_{\alpha_a}(x,y)$ are the Faddeev amplitudes obtained after solving the corresponding He trimer bound state problem, whereas E_{He_3} is its ground state energy; $\hat{n}_{l_z}(k_{\alpha_a}z)$ and $\hat{j}_{l_z}(k_{\alpha_a}z)$ are regularized Riccati-Bessel functions. Equations (2) in conjunction with the appropriate boundary conditions define the set of equations to be solved. The numerical methods employed will be briefly explained in the next section.

Once the integrodifferential equations of the scattering problem are solved, one has two different ways to obtain the scattering observables. The easier one is to extract the scattering phases directly from the tail of the solution, by calculating the logarithmic derivative $\left(\frac{\partial_z \mathcal{F}^K_{\alpha_a}(x,y,z)}{\mathcal{F}^K_{\alpha_a}(x,y,z)}\right)$ of the open channel's K amplitude α_a in the asymptotic region:

$$\tan \delta = \frac{k_{\alpha_a}\hat{j}'_l(k_{\alpha_a}z) - \frac{\partial_z \mathcal{F}^K_{\alpha_a}(x,y,z)}{\mathcal{F}^K_{\alpha_a}(x,y,z)}\hat{j}_l(k_{\alpha_a}z)}{\frac{\partial_z \mathcal{F}^K_{\alpha_a}(x,y,z)}{\mathcal{F}^K_{\alpha_a}(x,y,z)}\hat{n}_l(k_{\alpha_a}z) - k_{\alpha_a}\hat{n}'_l(k_{\alpha_a}z)}. \tag{12}$$

This result can be independently verified by using an integral representation of the phase shifts

$$k_{\alpha_a}\tan \delta = -\frac{m}{\hbar^2}\int \Phi^{(123)}_{\alpha_a}\hat{j}_l(k_{\alpha_a}z)(V_{14} + V_{24} + V_{34})\Psi dV. \tag{13}$$

$\Phi^{(123)}_{\alpha_a}$ is the trimer—composed from the He atoms indexed by 1, 2, and 3—ground state w.f. normalized to unity and Ψ is normalized according to

$$\Psi(\vec{x}_i,\vec{y}_i,\vec{z}_i) = \Phi^{(123)}_{\alpha_a}(\vec{x},\vec{y})[\hat{j}_{l_z}(k_{\alpha_a}z) + \tan(\delta)\hat{n}_{l_z}(k_{\alpha_a}z)]. \tag{14}$$

Detailed discussions on this subject can be found in [25,26].

C. Numerical methods

In order to solve the set of integrodifferential equations—obtained when projecting Eq. (2) and the appropriate bound-

TABLE I. Convergence of He trimer calculations obtained when increasing partial wave basis. In the three columns are, respectively, presented trimer ground (B_3) and excited (B_3^*) state energies in mK, as well as atom-dimer scattering length ($a_0^{(2+1)}$) in Å.

l_{max}	B_3 (mK)	B_3^* (mK)	$a_0^{(1+2)}$ (Å)
0	89.01	2.0093	155.39
2	120.67	2.2298	120.95
4	125.48	2.2622	116.37
6	126.20	2.2669	115.72
8	126.34	2.2677	115.61
10	126.37	2.2679	115.58
12	126.39	2.2680	115.56
14	126.39	2.2680	115.56

ary conditions Eqs. (8)–(11) into a partial wave basis—the components $\mathcal{F}^\alpha_i$ are expanded in terms of piecewise Hermite spline basis:

$$\mathcal{F}^\alpha_i(x,y,z) = \sum c^\alpha_{ijkl}S_j(x)S_k(y)S_l(z).$$

We use piecewise Hermite polynomials as a spline basis. In this way, the integrodifferential equations are converted into an equivalent linear algebra problem with unknown spline expansion coefficients to be determined. For bound states, the eigenvalue-eigenvector problem reads

$$Ax = EBx, \tag{15}$$

where A and B are square matrices, while E and x are, respectively, the unknown eigenvalue(s) and its eigenvector(s). In the case of the elastic scattering problem, a system of linear algebra equations is obtained:

$$[A - E_{cm}B]x = b, \tag{16}$$

where x is a vector of unknown spline expansion coefficients and b is an inhomogeneous term, generated when implementing the boundary conditions Eq. (11). For detailed discussions on the equations and method used to solve large scale linear algebra problems, one can refer to [26].

III. TRIMER SCATTERING AND BOUND STATES

As mentioned in the Introduction, trimer states have been broadly explored in many theoretical works. Hyperspherical, variational and Faddeev techniques were used to calculate accurately bound state energies [16,17,19,27–30] as well as to test different He-He interaction models. Nevertheless, we found it useful to consider these states as a first step, before the more ambitious analysis of He tetramer states could be undertaken. Special emphasis will be attributed to He-He$_2$ scattering calculations, which are less studied and for which some discrepancies were pointed out [18,19]. Some arguments will also be developed in favor of considering the first trimer excitation as an Efimov state.

We present in Table I the convergence of the He trimer states as a function of the partial-wave basis size. It contains results for the ground (B_3) and first excited (B_3^*) state binding

TABLE II. Mean values for He trimer ground and excited states. In this table B, T, and V indicate, respectively, binding, mean kinetic, and potential energies calculated in mK; x_{ij} stands for interparticle distance.

	Ground state		Excited state	
B (mK)	126.39	126.4 [17]	2.268	2.265 [17]
$\langle T \rangle$ (mK)	1658	1660 [17]	122.1	121.9 [17]
$\langle V \rangle$ (mK)	−1785	−1787 [17]	−124.5	−124.2 [17]
$\sqrt{\langle x_{ij}^2 \rangle}$ (Å)	10.95	10.96 [17]	104.3	102.7 [30]
$\langle x_{ij} \rangle$ (Å)	9.612	9.636 [17]	83.53	83.08 [17]
$\langle x_{ij}^{-1} \rangle$ (Å^{-1})	0.135		0.0267	
$\langle x_{ij}^{-2} \rangle$ (Å^{-2})	0.0230	0.0233 [31]	0.00218	

energies as well as for the He-He$_2$ scattering length ($a_0^{(1+2)}$). The basis truncations were made by limiting partial angular momentum values, applying selection criteria $l_x = l_y \leqslant l_{max}$. One can remark that the convergence is monotonic and quite similar for the He$_3$ bound states and for the He-He$_2$ scattering length calculations. These results demonstrate that in order to ensure five digit accuracy, the partial wave basis must include FY amplitudes with angular momentum values up to 12. However, for reaching a 1% accuracy, $l_{max} = 4$ turns out to be enough.

In Table II are summarized some relevant properties of the trimer ground and excited states. Together with their binding energies (B) we give some average quantities like kinetic $\langle T \rangle$ and potential energy $\langle V \rangle$ values and moments of interparticle distances x_{ij}. Our results are in perfect agreement with other existing calculations [17,29,30]; the most accurate of them have been included in this table for comparison.

The situation is more ambiguous for the He-He$_2$ scattering length a_0. Results obtained by Sandhas *et al.* [16]—solving Faddeev equations—and Blume *et al.* [29]—using hyperspherical harmonics—agreed with each other on a scattering length value $a_0 = 126$ Å. However, Roudnev [18], using also Faddeev equations, found a smaller value $a_0 = 115.4 \pm 0.1$ Å. It seems that in the Sandhas *et al.* [16] calculation a relatively small grid was employed, which did not allow one to disentangle the contribution of the virtual dimer break up component in the asymptotic behavior of the wave function. A more recent study [19] of the same authors provided a value of $a_0 = 115.5 \pm 0.5$ Å, in full agreement with Roudnev's result.

Our calculations are also very close to this value. When using a numerical grid limited to $y_{max} = 450$ Å we obtain $a_0 = 134$ Å, still far from the final result. Note that hyperradial grids employed in [16] were limited to $\rho_{max} = \sqrt{x^2 + y^2} = 460$ Å. The results of Table I have been obtained using a grid with $y_{max} = 950$ Å, i.e., He-He$_2$ distance $r_{max} = \frac{\sqrt{3}}{2} y_{max} = 823$ Å, which is large enough to reduce the grid-dependent variations to the fourth significant digit. As a function of r_{max}, the scattering length varies smoothly (see Fig. 2) and converges towards the value $a_0(\infty) = 115.2$ Å, very close to the one given by Roudnev, $a_0 = 115.4 \pm 0.1$ Å.

Whether or not the trimer first excitation is an Efimov [10] state has been an issue of strong polemics [32,33]. In
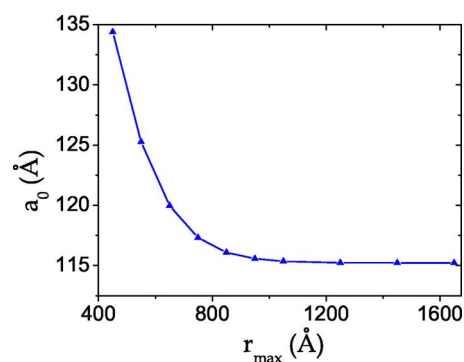
FIG. 2. (Color online) Convergence of He-(He)$_2$ scattering length obtained when enlarging the solution domain of Faddeev equations in He-(He)$_2$ separation direction (variable y) with additional discretization points.

fact, when using effective range theory and describing the system by zero-range interactions, it is not difficult to show the appearance of an Efimov state. However, the problem becomes complicated in calculations with finite range potentials. Efimov states accumulate according to a logarithmic law

$$N \approx \frac{1}{\pi} \ln \frac{|a|}{r_0}$$

and thus the two body scattering length should each be time increased by a factor $\sim e^{\pi} \approx 23$ (or the dimer binding energy reduced $\sim e^{2\pi} \approx 530$ times) to allow the appearance of an additional Efimov state. To handle this property, the grids employed in calculations should be extremely large and dense, capable on one hand to accommodate extended wave functions, and on the other hand to trace the very weak binding of the third particle to the dimer. Such requirements cannot be fulfilled in the calculations with realistic interactions. Thus the basic clue in claiming excited trimer to be an Efimov state is the fact that this state disappears when the interatomic potential is made less attractive [15,34,35]. Actually, if this potential is multiplied by an enhancement factor $\gamma > 1$ then the following effect is observed: first, the difference between the trimer excited state binding energy (B_3^*) and the dimer one (B_2) increases with γ. Then, for larger values of γ the difference ($B_3^* - B_2$) monotonously decreases and for $\gamma > 1.2$ the trimer excited state moves below the dimer threshold and becomes a virtual one.

The demonstration of the Efimov effect can be accomplished only by showing accumulation of new states when dimer binding energy decreases. Such a demonstration has been given in Ref. [36] using semiempirical potential HFD-B [6]. We would like to remark that the formation of new states can be alternatively demonstrated by studying the γ-dependence of the three-body scattering length, without the necessity of solving the bound state problem. In scattering calculations, the numerical solution of three-body equations can be reduced to the interaction domain and the wave function extended outside this region using analytical expressions [37].
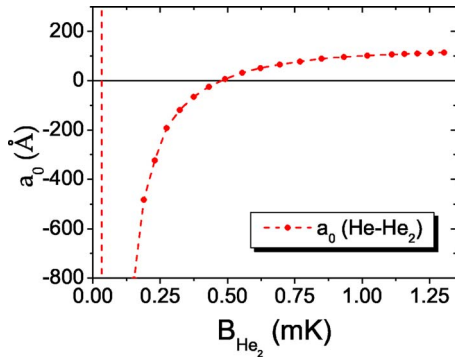
FIG. 3. (Color online) The change of the atom-dimer scattering length as a function of the dimer binding energy.

TABLE III. Convergence of the He tetramer calculations obtained when increasing the partial wave basis of Eq. (7). The two columns represent, respectively, the tetramer ground state binding energy in mK (B_4) and the atom-trimer scattering length ($a_0^{(3+1)}$) in Å.

max (lx, ly, lz)	B_4 (mK)	$a_0^{(3+1)}$ (Å)
0	348.8	≈ -855
2	505.9	190.6
4	548.6	111.6
6	556.0	105.9
8	557.7	103.7

In Fig. 3 we display the behavior of the He-He$_2$ scattering lengths, when the He-He potential is multiplied by a scaling factor $\gamma < 1$, according to $\widetilde{V} = \gamma V$. In this figure, the He-He$_2$ scattering length is plotted as a function of the fictive dimer binding energy. One can see that, when decreasing γ, scattering length decreases. However, in the absence of Efimov states one should expect them increasing, since reducing γ, the dimer target becomes larger. Once γ is reduced to ≈ 0.990, the scattering length becomes negative and for values $\gamma \approx 0.979$ it exhibits a singularity going from $a_0 = -\infty$ to $+\infty$. This singularity corresponds to the appearance of a new trimer bound state (i.e., second excited state in He trimer). This analysis clearly demonstrates that the He trimer excited state is an Efimov one. It is worth mentioning that for an enhancement factor $\gamma = 0.979$, the He dimer binding energy is only 0.046 mK.

IV. TETRAMER STATES

The major aim of this paper is to provide a comprehensive analysis of the four-atomic He compound (tetramer). The first efforts to describe this system were made already in the late 1970s by Nakaichi *et al.* [38] using a variational method. Later on, variational Monte Carlo techniques were used by several authors [29,39–41] to compute the tetramer ground state. These methods are very powerful in calculating $L^\Pi = 0^+$ bound state properties, but are seldom generalized to describe excited states and are not appropriate for the scattering problem.

FY techniques were also used by Nakaichi *et al.* [42] to calculate the tetramer ground state binding energy and the He-He$_3$ scattering length. However, in order to reduce the—at that time—outmatching numerical costs, some important approximations were made. The He-He potential was restricted to S-wave and written as a one-rank separable expansion and the same expansion was used to represent the FY amplitudes. These approximations led to a tetramer ground state which is underbound by 40% with respect to their own variational result [38]. A recent attempt to calculate the He tetramer binding energy using S-wave FY equations was done in [43], although without separable expansion of FY amplitudes.

The FY calculations we present here contain no approximation other than the finite basis set used in the partial wave

expansion (7). This basis set included amplitudes with internal angular momentum not exceeding a given fixed value l_{max}, i.e., fulfilling the condition $\max(l_x, l_y, l_z) \le l_{max}$. The largest basis we have considered has $l_{max} = 8$, and consists of 180 FY amplitudes, a number by two orders of magnitude larger than in preceding calculations. Note that the smallest basis, which is often referred to as S-wave approximation, is obtained by fixing $l_{max} = 0$ and requires only two amplitudes, one of type K and one of type H. The convergence is displayed in Table III for the tetramer ground state binding energy and He-He$_3$ scattering length.

The corresponding FY K-amplitudes are displayed in Fig. 4 as a function of the He-He$_3$ distance $r = \sqrt{\frac{2}{3}} z$. One can see the different scales involved in the bound state and zero energy scattering wave function.

The convergence of the tetramer calculations is sensibly slower than the one observed for the trimer case (see Table I). Such a deterioration is due to the complex structure of the involved FY components. Indeed, each He atom pair brings an additional hard-core region; the ensemble of these regions crosses over in the multidimensional configuration space [48] and results into a single domain with nontrivial geometry. Inside this multidimensional domain, the total wave function must vanish by cancelling the contributions of the different FY amplitudes, which can be achieved only at the price of increasing its functional complexity.
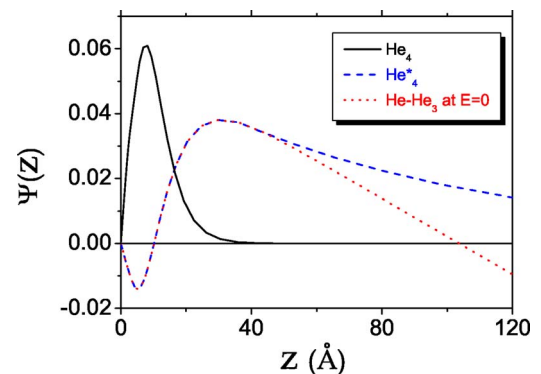
FIG. 4. (Color online) Comparison of the functional dependence of K-type FY components in one He atom separation from He$_3$ core direction. Single, dashed, and dotted line curves correspond, respectively, to tetramer ground, excited state, and He-He$_3$ zero energy scattering wave functions.

The convergence of the He-He$_3$ scattering calculations is also slightly slower than for tetramer ground state. This is a consequence of the scattering wave function, which presents a richer structure than the ground state one, as can be seen in Fig. 4. Tetramer ground state has a rather simple geometry: the four He atoms minimize their total energy by forming a tetrahedron. The total energy of the 1+3 scattering state ($E \approx -126$ mK) is considerably larger than the ground state one ($E \approx -558$ mK) and provides more flexibility to each atom. Furthermore, since the scattering length value is much larger than the size of the trimer target, the scattering wave function turns to be strongly asymmetric.

Despite these difficulties, the PW basis we have used enables one to reach rather accurate results: the tetramer ground state binding energy is converged up to 0.4%, while the final variation of the scattering length does not exceed 2%. Our best result for the ground state binding energy of He$_4$, B=558 mK, is in perfect agreement with the B=559(1) mK value, provided by several variational Monte Carlo techniques [29,39,40].

It is interesting to compare the bound state result with the effective field theory (EFT) predictions. It follows from this approach that systems governed by large scattering lengths should exhibit universal properties. The wave functions of such systems have very large extensions with only a negligible part located inside the interaction region. The detailed form of the short-range potential does not matter, since the system probes it only globally. It should be therefore possible to describe its action using only a few independent parameters (physical scales). One scale is obviously required to fix the two-body binding energy or the scattering length. Keeping fixed the two-boson binding energy, the three bosons system would collapse if the interaction range tends to zero, a collapse known as the Thomas effect [44]. This indicates that the three-body system is sensitive to an additional scale, which can be determined by fixing one three-body observable (for instance, the 3-particle binding energy or the 1+2 scattering length) [45,46].

It seems [14] that the four-boson binding energies remains finite if none of its three-boson subsystems collapse. Furthermore four- and three-body binding energies are found to be correlated [14]. The simplest way to establish such a correlation law is by using contact interactions. In this way, the two-body binding energy is fixed by the parameter strength of zero-range two-body force, whereas the three-body collapse is avoided and its binding energy is fixed by introducing a repulsive three-body contact term. Using this model Platter *et al.* [14] demonstrated that inside quite a large domain of dimer-trimer binding energy ratio (B_2/B_3), the correlation between tetramer and trimer binding energies is almost linear. In the same study, a numerical approximation of this correlation law was obtained.

If we take our dimers (B_{He_2}=1.30348 mK) and trimers binding energies as the scales for EFT with contact interaction, one obtains a tetramer binding energy of 485 and 491 mK, respectively, depending on which trimer energy— ground or excited—is used. This result is only by 13% smaller than our most accurate result.

One should remark that the EFT scaling laws are derived using contact interactions, which act only in S-wave. There-fore it would be more consistent to compare our values obtained using S-wave approximation (l_{max}=0). In this case, the EFT formulas give, respectively, B_{He_4}=330 and 325 mK depending on which trimer fixes the scale. These values must be compared with our result B_{He_4}=348.8 mK, i.e., EFT is only off by 6%.

The good agreement between exact and EFT results proves the great prediction power of the last approach. EFT works surprisingly well even beyond its natural limit of applicability: systems with a size significantly exceeding the range of interaction. Note, indeed, that the He tetramer and trimer ground states are rather compact objects, in which the interatomic separation is about $\approx$10 Å, and therefore comparable with He-He interaction range $\sim$3 Å.

Let us discuss now the He-He$_3$ scattering results. Nakaichi *et al.* [42], using S-wave separable expansion of the outdated HFDHE2 potential, obtained a large and negative scattering length a_0=−116 Å. Using the same HFDHE2 potential and restricting to l_{max}=0 amplitudes we have got also a negative, although much larger, scattering length value $a_0 \approx -5600$ Å. This result is, however, very unstable, as a consequence of the l_{max}=0 basis inability to describe the nontrivial behavior of the FY components in the hard-core region. If we add max(l_y, l_z)$\leq$4 amplitudes, the scattering length reduces to $\approx$−898 Å for the same HFDHE2 interaction model limited to S-wave. Similar calculations with the LM2M2 potential give $a_0 \approx -450$ Å. As one can see in Table III, the full potential must be used in order to obtain converged results. The presence of He-He interaction in higher partial waves cardinally changes the physics of He tetramer: not only the size but also the sign of the resonant scattering length changes, thus indicating the emergence of a new excited state in this compound.

Another effort to evaluate He-He$_3$ scattering length was made by Blume *et al.* [29]. In their work, effective He-He$_n$ potentials were constructed starting from the same LM2M2 He-He interaction model. Without taking into account the particle correlations, Blume *et al.* provided a positive He-He$_3$ scattering length a_0=56.1 Å.

As already mentioned, the large positive scattering length indicates the presence of a tetramer excitation close to the trimer ground state threshold. Much physics about this tetramer state can be learned by studying the behavior of the zero energy 1+3 scattering w.f., or what is even more practical, its FY components. These components are only partially symmetrized and have a more transparent asymptotic behavior [23,47]. The structure of the K-type FY component displayed in Fig. 4 proves that this state is the first tetramer excited state: the corresponding open channel FY amplitudes have two nodes in z, the He-He$_3$ separation direction. The first node is situated at $\approx$10 Å, i.e., inside the He$_3$ cluster, indicating the presence of a compact ground state. The second node is situated at $\approx$103.7 Å, which coincides with the scattering length value. This coincidence is not accidental: at such He-He$_3$ separations, the single He atom is already out of the interaction domain of the He$_3$ cluster. Close to this node, the FY components reach the well-known linear behavior:

$$\mathcal{F}^K_{\alpha_a}(x,y,z) \sim \phi_{He_3}(x,y)\left(\sqrt{\frac{2}{3}}z - a_0\right). \tag{17}$$

The factor $\sqrt{\frac{2}{3}}$ in front of the z-coordinate is due to mass scaling of Jacobi variables Eq. (4).

A direct calculation of the He_4 excited state represents nowadays a hardly realizable numerical task. This state is very weakly bound and its wave function very extended. In order to numerically reproduce it, one is obliged to use a very large and dense grid. On the other hand, one should be able to ensure a high accuracy to trace a small binding energy difference. For the time being, it constitutes an insurmountable obstacle in the context of the large computing power demanding four-body calculations.

Nevertheless the vicinity of the tetramers excited state to the He-He$_3$ continuum makes possible the extraction of its binding energy from the scattering results. A bound state is identified with a S-matrix $S_l(k)$ pole on the positive imaginary axis of the complex momentum plane. Since $S_l(k)$ is unitary, its general form close to the pole $k=ik_0$ is

$$S_l(k) = \frac{k + ik_0}{k - ik_0} = e^{2i\delta}. \tag{18}$$

The momentum k_0 is related to the tetramer binding energy measured with respect to trimer ground state threshold by $\Delta B_0 = \frac{\hbar^2 k_0^2}{2\mu_{3+1}}$, where $\mu_{3+1}=3m/4$ is the reduced atom-trimer mass.

On the other hand, the well-known effective range expansion can be used to approximate the low energy phase shifts:

$$k^{2l+1} \operatorname{ctg} \delta = -\frac{1}{a_l} + \frac{1}{2}r_l k^2 + o(k^2). \tag{19}$$

Combining relations (18) and (19), one obtains an expression for the bound state momentum k_0 in terms of the low energy parameters. For the He-He$_3$ scattering states with $l_z=0$, it reads:

$$\frac{1}{2}r_0 k_0^2 - k_0 + \frac{1}{a_0} = 0. \tag{20}$$

It follows from Eq. (20) that in order to obtain the unknown binding energy it is sufficient to know the low energy coefficients a_0 and r_0. The scattering length value a_0 has been already determined and the effective range r_0 can be extracted by fitting with Eq. (19) the He-He$_3$ low energies phase shifts. The corresponding extrapolation procedure is illustrated in Fig. 5. One can see that inside the considered momentum region, close to $k=|k_0|$, the effective range expansion works perfectly well. The obtained binding energy, $\Delta B_0=1.087$ mK, should not suffer much from higher order momentum terms in the expansion (19). Nevertheless, the He-He$_3$ effective range is pretty large, $r_0=29.1$ Å, and influences significantly the extrapolated binding energy value. By ignoring this term, one would get
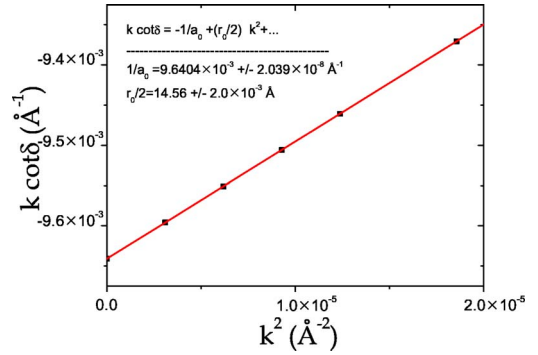
FIG. 5. (Color online) Extrapolation of He tetramer excited state binding energy from the He-He$_3$ scattering calculations. Low energy phase shift fit is made for k ctg δ values as a linear function of momentum squared (k^2).

$$\Delta B_0^{(0)} = \frac{\hbar^2}{2\mu_{3+1}a_0^2}, \tag{21}$$

and a binding energy of only $\Delta B_0^{(0)}=0.751$ mK will be obtained, i.e., a value by 30% smaller.

We finally predict the existence of a $L^{\Pi}=0^+$ tetramer excited state with binding energy $B^*_{He_4}=\Delta B_0+B_{He_3}=127.5$ mK. This value compares well with the EFT prediction [14] discussed above, which gives the range $B^*_{He_4} \in [128–130]$ mK, a dispersion due to the fact that the interpolation was done for the total binding energy and not the sensibly smaller relative value ΔB_0.

The validity of the procedure we use to obtain the binding energy of the excited tetramer can be verified in the dimer case, for which direct bound state calculations causes no difficulty. The procedure is illustrated in Fig. 6. The accurate dimer binding energy is $B_{He_2}=1.30348$ mK, a value very close to $\Delta B_0=1.087$ mK, and allows one to control the inaccuracy made when disregarding higher order terms in expansion (19). By considering only two terms in the expansion (19) we have got $B_{He_2}=1.3036$ mK, only differing in the fifth significant digit from the directly calculated value. In addition, the He-He potential effective range extracted by fitting the low energy phase shift is $r_0=7.337$ Å. This value can be independently calculated applying the Wigner formulas from
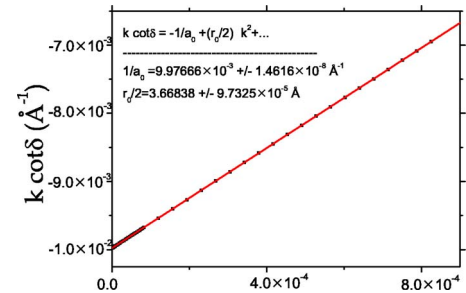
FIG. 6. (Color online) He dimer binding energy extrapolated from He-He scattering calculations. Low energy phase shift k ctg δ is fitted with a linear function of k^2. Exact k ctg $\delta(k^2)$ values are indistinguishable from the linear fit.

the zero-energy scattering wave function, which gives $r_0 = 7.326$ Å, in nice agreement with the extrapolated one. Such an agreement demonstrates the validity of our approach.

One should, however, mention that the very same procedure is not applicable to the trimer excited state calculation. If done, it would lead to a complex momentum $k_0 = (1.3 \pm 0.8i) \times 10^{-2}$ Å^{-1}. This is a consequence of a dimer binding energy almost as small as $\Delta B^*_{\text{He}_3} = B^*_{\text{He}_3} - B_{\text{He}_2}$. In this case, the scattering phase shifts are affected by two open thresholds and thus a single channel S-matrix theory is not appropriate. In He-He$_3$ scattering, the nearest threshold He$_2$-He$_2$ opens only for scattering energies $E_{cm} \approx 124$ mK and thus is well separated from the energy region of interest (~ 1 mK).

It is interesting to compare the effective ranges for He-He, He-He$_2$, and He-He$_3$ systems. They are, respectively, $r_0 = 7.33$, 79.0, and 29.1 Å. It is not surprising that the atom-dimer effective range is the largest one: this is a consequence of a dimer ground state which is the most extended of the three considered targets. The atom-trimer effective range is more than a third of the atom-dimer one and is significantly larger than the range of the He-He potential. This suggest that the trimer ground state has a structure with a sizable probability to find single He atoms separated by 20–30 Å apart from its center.

We can still use the He-He$_3$ scattering w.f. to obtain a relatively good description of the tetramer excited state. In fact, the left-hand side of FY Eqs. 2 for the bound and zero-energy He-He$_3$ state differ only by a small energy term, which has a little effect on the w.f. inside the interaction region, dominated by large kinetic and potential terms. These functions sensibly differ only in the He-He$_3$ asymptotes, where they can be described analytically [23,47] as a tensor product of a strongly bound trimer in its ground state and a plane wave of the remaining He atom with energy $E - E_{\text{He}_3}$. In practice, the two w.f. differ only by FY amplitudes contributing to the open channels. For zero-energy scattering, one has a linearly diverging open channel FY amplitude as described in Eq. (17). For a bound state these amplitudes converge very slowly with a small exponential factor:

$$\mathcal{F}^K_{\alpha_a}(x,y,z) \sim \phi_{\text{He}_3}(x,y) e^{-\sqrt{2/3}k_0 z}. \tag{22}$$

The closed channel FY amplitudes rapidly vanish being shrunken by a relatively large $e^{-\rho\sqrt{mB_{\text{He}_3}/\hbar^2}}$ exponent, with $\rho = \sqrt{x^2+y^2+z^2}$.

Using this approximation for the tetramer excited state wave function, we have calculated some of its properties, which are summarized in Table IV.

V. TETRAMER AND TRIMER ROTATIONAL STATES

Considering that ^{4}He is a spinless atom, the rotational states of ^{4}He-multimers can be classified according to their parity (Π) and total orbital angular momentum (L). FY components are very useful to classify these states as well as to analyze their properties. As we have mentioned in Sec. II, the l_x quantum number must be even (see Fig. 7). It follows that for He trimer, the $L^\Pi = 0^-$ states are forbidden. Further we

TABLE IV. Mean values for He tetramer ground and excited states. In this table B, T, and V indicates, respectively, binding, mean kinetic, and potential energies calculated in mK; x_{ij} stands for interparticle distance.

	Ground state		Excited state	
B (mK)	557.7	559 [40]	127.5	128–130 [14]
T (mK)	4107		1900	
V (mK)	−4665	−4850 [40]	−1913	
$\sqrt{\langle x_{ij}^2 \rangle}$ (Å)	8.40		34.4	
$\langle x_{ij} \rangle$ (Å)	7.69	7.76 [40]	24.8	
$\langle x_{ij}^{-1} \rangle$ (Å^{-1})	0.156		0.088	
$\langle x_{ij}^{-2} \rangle$ (Å^{-2})	0.0286	0.0251 [31]	0.013	

classify the He trimer states into those which can break into dimer and a freely propagating He atom, and those in which dimer states are forbidden by symmetry requirements. In the first group, we have states with $L^\Pi = (1^-, 2^+, 3^-, \ldots)$. To be decay stable, these states should be more bound than dimer. The other group is formed by the $L^\Pi = (1^+, 2^-, 3^+, \ldots)$ states, which can only break into three helium atoms.

Clearly, the 1^- is the most promising candidate for a trimer stable rotational state. This state is realized with the smallest partial angular momentum, i.e., $l_x + l_y \geqslant 1$, and consequently contains the smaller centrifugal terms in the Hamiltonian. The nonexistence of this state would imply the nonexistence of other states of the same decay group, i.e., $L^\Pi = (1^-, 2^+, 3^-, \ldots)$, since they involve larger centrifugal energies: $l_x + l_y \geqslant 2$. The existence of stable trimers in the second group is very doubtful; the most favorable would be the 2^- one, for which one has already $l_x + l_y \geqslant 3$.

In a similar way, we can classify the rotational states of He tetramer (see Fig. 1). In the first group, we have states $L^\Pi = (1^-, 2^+, 3^-, \ldots)$ for which the first decay threshold is the trimer ground state. The most promising state inside this group is the 1^- one. For this state, the condition $l_x + l_y + l_z \geqslant 1$ must be satisfied.

In the second group, we have trimer decay stable states $L^\Pi = (1^+, 2^-, 3^+, \ldots)$. These states can neither break into trimer-atom pair nor into two dimers: their reference threshold is dimer plus two free atoms. The $L^\Pi = 0^-$ state represents a special case: it can be broken only into four free atoms.
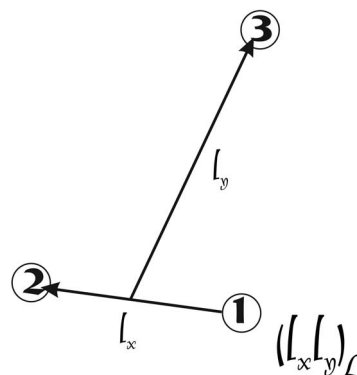
FIG. 7. Coupling scheme for three-particle FY component.

The FY formalism we are using allows one to calculate multiparticle rotational states with the same ease as zero angular momentum ones. However, none of trimer or tetramer rotational states have been found stable. The nonexistence of weakly bound states can be easily verified using low energy scattering techniques for trimer and tetramer states in the first decay groups (two cluster). In addition, the calculated scattering length turns out to be an indicator for the strength of the interaction between the scattered clusters and thus tests if near-threshold bound or resonant states are present.

For atom-dimer scattering in 1^-, one obtains a large positive scattering length $(a_1)^{1/3} = 114.2$ Å. If He-He interaction is changed, this length scales with the dimer size. If we add a small attractive three-body interaction to force a trimer binding without affecting dimer, this scattering length becomes smaller. In fact, when the attractive three-body force is weak, this scattering length reduces very slowly. Only when this additional force becomes rather strong, close to the critical value binding 1^- trimer, the scattering length falls down to $-\infty$. It crosses a singularity, passing from $-\infty$ to $+\infty$ at the value where 1^- trimer bound state appears, and then again stabilizes to large positive value. This clearly indicates that no trimer rotational state exist with quantum numbers $L^\Pi = (1^-, 2^+, 3^-, \dots)$. An even much stronger attractive three-body force is required to bind the second group $L^\Pi = (1^+, 2^-, 3^+, \dots)$ states, thus excluding the possible existence of bound or even near-threshold resonant He trimer states.

The case of rotational tetramers is identical to the trimers one. A positive scattering length $(a_1)^{1/3} \approx 12.28$ Å is also obtained for He-He$_3$ scattering with $L^\Pi = 1^-$. This value is sensibly smaller than the one for 1^- atom-dimer scattering, which simply results from the scaling with the target size. As in trimers case, one has to apply a strong additional attractive force to reduce this scattering length to $-\infty$, i.e., to force the 1^- tetramers binding. Tetramers in the second decay group, as well as $L^\Pi = 0^-$, seem to be even less favorable: they require an even stronger additional force to be bound. We conclude therefore that no bound or even near-threshold resonant states should exist for tetramers with $L^\Pi \neq 0^+$.

VI. SUMMARY

In this paper, we have outlined Faddeev-Yakubovski equation formalism in configuration space. It enables a consistent description of bound and scattering states in multiparticle systems. This formalism was applied to study the lightest ($N=2,3,4$) systems of He atoms using realistic He-He interaction. We have presented accurate calculations for bound He trimer and tetramer states, as well as for low energy atom-dimer and atom-trimer scattering.

Our main results concern the He tetramer states. We have obtained a tetramer ground state binding energy of $B = 558$ mK, in perfect agreement with the most accurate variational results.

The first realistic calculation of He-He$_3$ scattering length has been achieved, with the prediction $a_0 = 104$ Å. Such a large value indicates the existence of a tetramer excited state close to the trimer ground state threshold.

Its binding energy can hardly be determined in a direct bound state calculation, due to the difficulties in accommodating a very extended wave function. We have shown that this energy can be obtained by applying an effective range expansion to low energy $1+3$ scattering states. We predict the existence of a $L^\Pi = 0^+$ He tetramer excited state with a binding energy of 127.5 mK, situated 1.09 mK below the trimer ground state.

Finally, we have studied the possible existence of rotational states in three and four atomic He compounds. It has been shown that neither the He trimer nor the tetramer have bound rotational ($L^\Pi \neq 0^+$) states. The existence of corresponding near-threshold resonances is also doubtful.

[1] S. Datz, G. W. F. Drake, T. F. Gallagher, H. Kleinpoppen, and G. zu Putlitz, Rev. Mod. Phys. **71**, S223 (1999).

[2] F. Luo, G. C. McBane, G. Kim, C. F. Giese, and W. R. Gentry, J. Chem. Phys. **98**, 3564 (1993).

[3] W. Schollkopf and J. P. Toennies, Science **266**, 1345 (1994).

[4] R. A. Aziz and M. J. Slaman, J. Chem. Phys. **94**, 8047 (1991).

[5] A. R. Janzen and R. A. Aziz, J. Chem. Phys. **103**, 9626 (1995).

[6] R. A. Aziz, F. R. W. McCourt, and C. C. K. Wong, Mol. Phys. **61**, 1487 (1987).

[7] R. A. Aziz and M. J. Slaman, J. Chem. Phys. **94**, 8047 (1991).

[8] K. T. Tang, J. P. Toennies and C. L. Yiu, Phys. Rev. Lett. **74**, 1546 (1995).

[9] A. R. Janzen and R. A. Aziz, J. Chem. Phys. **107**, 914 (1997).

[10] V. Efimov, Phys. Lett. **33**(B), 563 (1970); Nucl. Phys. A **210**, 157 (1973).

[11] D. B. Kaplan, e-print nucl-th/9506035.

[12] G. P. Lepage, e-print nucl-th/9706029.

[13] E. Braaten and H. W. Hammer, Phys. Rep. **428**, 259 (2006), and references therein.

[14] L. Platter, H. W. Hammer, and Ulf-G. Meissner, Phys. Rev. A **70**, 052101 (2004).

[15] T. Cornelius and W. Glöckle, J. Chem. Phys. **85**, 3906 (1986).

[16] A. K. Motovilov, W. Sandhas, S. A. Sofianos, and E. A. Kolganova, Eur. Phys. J. D **13**, 33 (2001).

[17] P. Barletta and A. Kievsky, Phys. Rev. A **64**, 042514 (2001).

[18] V. Roudnev, Chem. Phys. Lett. **367**, 95 (2003).

[19] E. A. Kolganova, A. K. Motovilov, and W. Sandhas, Phys. Rev. A **70**, 052711 (2004).

[20] L. D. Faddeev, Zh. Eksp. Teor. Fiz. **39**, 1459 (1960) [Sov. Phys. JETP **12**, 1014 (1961)].

[21] O. A. Yakubowsky, Sov. J. Nucl. Phys. **5**, 937 (1967).

[22] S. P. Merkuriev and S. D. Yakovlev, Theor. Math. Phys. **56**, 60 (1983).

[23] S. P. Merkuriev and L. D. Faddeev, *Quantum Scattering Theory for Systems of Several Particles* (Kluwer Academic Publishers, Dordrecht, 1993).

[24] S. P. Merkuriev, A. K. Motovilov, and S. D. Yakovlev, Theor. Math. Phys. **94**, 435 (1993).

[25] F. Ciesielski, Thèse Univ. J. Fourier (Grenoble), 1997.

[26] R. Lazauskas, Ph.D. thesis, Université Joseph Fourier, Grenoble, 2003; http://tel.ccsd.cnrs.fr/documents/archives0/00/00/41/78/.

[27] J. Carbonell, C. Gignoux, and S. P. Merkuriev, Few-Body Syst. **15**, 15 (1993).

[28] E. Nielsen, D. V. Fedorov, and A. S. Jensen, J. Phys. B **31**, 4085 (1998).

[29] D. Blume and Chris H. Greene, J. Chem. Phys. **112**, 8053 (2000).

[30] V. Roudnev and S. Yakovlev, Chem. Phys. Lett. **328**, 97 (2000).

[31] A. Kalinin, O. Kornilov, L. Rusin, J. P. Toennies, and G. Vladimirov, Phys. Rev. Lett. **93**, 163402 (2004).

[32] T. Gonz'alez-Lezana, J. Rubayo-Soneira, S. Miret-Artes, F. A. Gianturco, G. Delgado-Barrio, and P. Villarreal, Phys. Rev. Lett. **82**, 1648 (1999).

[33] B. D. Esry, C. D. Lin, C. H. Greene, and D. Blume, Phys. Rev. Lett. **86**, 4189 (2001).

[34] B. D. Esry, C. D. Lin, and C. H. Greene, Phys. Rev. A **54**, 394 (1996).

[35] E. Nielsen, D. V. Fedorov, and A. S. Jensen, Phys. Rev. Lett. **82**, 2844 (1999).

[36] E. A. Kolganova and A. K. Motovilov, Phys. At. Nucl. **62**, 1179 (1999).

[37] J. Carbonell and C. Gignoux, Few-Body Syst., Suppl. **7**, 270 (1994).

[38] S. Nakaichi, Y. Akaishi, H. Tanaka, and T. K. Lim, Phys. Lett. **68**A, 36 (1978).

[39] D. Bressanini, M. Zavaglia, M. Mellab, and G. Morosic, J. Chem. Phys. **112**, 717 (2000).

[40] M. Lewerenz, J. Chem. Phys. **106**, 4596 (1997).

[41] R. Guardiola, M. Portesi, and J. Navarroa, Phys. Rev. B **60**, 6288 (1999).

[42] S. Nakaichi, T. K. Lim, Y. Akaishi, and H. Tanaka, Phys. Rev. A **26**, 32 (1982); S. Nakaichi-Maeda and T. K. Lim, Phys. Rev. A **28**, 692 (1983).

[43] I. N. Filikhin1, S. L. Yakovlev, V. A. Roudnev, and B. Vlahovic, J. Phys. B **35**, 501 (2002).

[44] L. H. Thomas, Phys. Rev. **47**, 903 (1935).

[45] A. E. A. Amorim, T. Frederico, and L. Tomio, Phys. Rev. C **56**, R2378 (1997).

[46] E. Nielsen, D. V. Fedorov, A. S. Jensen, and E. Garrido, Phys. Rep. **347**, 373 (2001).

[47] A. A. Kvitsinskii, Yu. A. Kuperin, and S. P. Merkuriev, Sov. J. Part. Nucl. **17**, 113 (1986).

[48] In the two particle case one has a single hard-core region in three-dimensional particle space; this region has simply a form of the sphere of radius r_{hc} placed at the origin. One has three hard-core conditions for a three-particle system; these regions are intersecting in six-dimensional multiparticle space. The four particle-case already has six hard-core conditions for nine-dimensional multiparticle space.